Chapter 18
Classification of Keratoconus Using Corneal Topography Pattern with Transfer Learning Approach

Savita R. Gandhi, Jigna Satani, and Dax Jain

Abstract Keratoconus, also referred as KCN, is a progressive ocular disease that causes the thinning of cornea and distorts its curvature. The gradual thinning of cornea induces the loss of elasticity results into a cone-shaped protrusion. This may irreversibly change the cornea and could cause the loss of vision. In spite of many researches have been pursued over a decade, it remains difficult to detect keratoconus accurately in its early stage. Apart from being an important prerequisite for refractive surgery, identification of corneal steepening shape helps to choose the right treatment and determines the progression of the keratoconus. The different shapes of steepening are extracted from the given corneal topographies herein. In this study, we have applied, pretrained deep learning models using transfer learning approach to classify the corneal topography patterns from corneal eroded images derived from the corneal images. The said models are used to classify corneal eroded images into ten labels as per patterns prevailed in corneal curvature due to the steepening of the surface. This is a step forward toward predicting the progression of KCN in its early stage with more accuracy.

Keywords Keratoconus · Corneal topography · ATLAS 9000 · Deep learning · Transfer learning · Pretrained ImageNet model · Computer vision · Edges with mask

18.1 Introduction

Keratoconus (KCN) is an ophthalmic condition wherein cornea bulges out conically due to progressive thinning of outer layer referred as cornea, leading to vision loss

S. R. Gandhi (✉) · J. Satani · D. Jain
Department of Computer Science, Gujarat University, Ahmedabad 380009, India
e-mail: drsavitagandhi@gmail.com

J. Satani
e-mail: jignasatani@gmail.com

D. Jain
e-mail: daxjain789@gmail.com

© The Author(s), under exclusive license to Springer Nature Singapore Pte Ltd. 2023

J. Choudrie et al. (eds.), *ICT with Intelligent Applications*, Smart Innovation, Systems and Technologies 311, https://doi.org/10.1007/978-981-19-3571-8_18

[1–3]. Various researches suggest that the factors such as sensitive or thin cornea, extensive eye rubbing, environmental condition, extensive screen time and genetic factors are some of the root causes of the disease [4]. Latest customized corneal lenses may halt the progression of the disease, subject to acceptance by the eyes. In severe cases of KCN, treatments like corneal transplantation and epithelium grafting are sometimes endangered in absence of any possible treatments [5–7].

Even with the advancement of technology, the early detection of KCN is yet the best remedy. Moreover, the refractive surgery is not advised on keratoconic eyes [8, 9]. The clinical screening of keratoconus is now replaced by the topographical screening using keratometry devices which produce a color topographic and tomographic map [9, 10]. These maps render measurement of corneal steepening. The incidences of corneal elevation and other irregularities are revealed in topographical maps [11] that elaborate the patterns as per the progression of the keratoconus. Thus, topographical display of various shapes plays an important role in determining the severity of the KCN along with other corneal measures. At least, as of now, it seems that the early identification of (a) shape, (b) steepening patterns and (c) thinning is the best way out, as, in most of the cases, KCN exhibits symptoms of its presence only in the later stages and by that time irreversible damages might occur. Even a small delay in determination of the KCN in its early stages may narrow down the choices of otherwise available appropriate treatments [12, 13].

In this study, the shape of corneal distortion manifested by the keratoconus has been detected by extracting a pattern of corneal irregularities from the given corneal topographical maps. These patterns were further classified by us into ten significant shapes associated with the progression of disease. Here, to determine these patterns, we primarily used (a) the 'transfer learning': an outshoot of deep layered network learning techniques, (b) tailoring CNN (convolutional neural network) and (c) pretrained ImageNet models along with the methodologies of (d) 'Computer Vision'. The topographic maps used here-in were axial curvature elevation maps, derived from the ATLAS 9000 topographer. The CNN being the best known deep learning neural network for image recognition, classification and detection of objects from the images by extracting features has been our obvious choice.

18.2 Related Work

The transfer learning is based upon conventional wisdom of 'sharing knowledge with others'. Using the data similar in nature but collected from different sources, the pretrained deep learning models are firstly trained rigorously and then these vastly knowledge equipped models are applied upon relatively smaller data or task to speed-up the very training [14, 15].

The application of the 'deep neural network' and 'transfer learning' upon medical images has proven its worth and hence are extensively used with MRI, CT scan, X-ray, microscopy, color fundus images, etc. [16].

Not, so long ago, the optic diseases were diagnosed primarily through clinical screening but the sharp advancement of neural network has drawn the attention of researchers for early and accurate detection of ophthalmic disease [17]. In past decades, many scientists have significantly contributed in keratoconus detection by applying NN, ANN, SVM, MLP, RBFNN, decision tree, etc. [10, 18–22]. Lately, introduction of machine learning techniques have empowered the process of identification and classification of disease including keratoconus [23, 24].

The convolution neural network has just begun to claim its efficiency over other peer techniques by giving higher accuracy in image recognition and classification, so does for keratoconus detection as well [25–28]. Lavric et al. [29] applied customized CNN architecture named as 'KeratoDetect' to detect the eyes with keratoconus by achieving 99% accuracy after increasing epoch numbers.

With the recent advancement in deep learning, a conventional thought of 'sharing gained knowledge' has been interpreted in transfer learning which allows a small-scale task to use the learnings of pretrained large-scale models such as AlexNet, DenseNet, ResiNet, VGG16, etc. Among family of pretrained models, VGG16 is simple, lightweight and shows efficient outcomes with image segregation. Kim et al. [16] suggested transfer learning approach to classify images between X-ray images and normal images by mapping databases of various sources where images were obtained from same imaging modalities. Salih et al. [30] performed CNN trained by VGG16 to extract the features from corneal topography which was supplied to SVM for classifying features of elevation and thickness. The classification outcome was further used to predict its match with clinical diagnosis of corneal disease.

Deep learning neural network alongside with the computer vision techniques offer tailor-made solution [31]. The study of the achievements of other researchers suggests the significant performance of the deep neural network [32–35], motivating us to apply it with the recent advance techniques of transfer learning for our research.

18.3 Study Data and Methods

Being an outperformer, the rich deep learning technique has delivered new approach of transferring the former learnings to new data and tasks, also referred as inductive transfer. Transfer learning applies previously gained knowledge to learn new tasks which may be smaller in size or used with imbalanced data. We customized convolutional neural network (CNN) to incorporate various pretrained ImageNet models to deal with corneal topographies used.

The bilateral axial elevation maps, clinically tested and approved, were used as the subject group. These maps were fetched from corneal wavefront analysis and Placido disk-based Carl Zeiss ATLAS9000 topography modality. This device has been mainly used to measure corneal shape, curvature and irregularities. The elevation-based topography has its own advantages over Placido-based devices [36, 37]. The axial curvature maps display global curvature of the corneal surface. Corneal topographical maps have been used to detect the keratoconus and identify the shapes of steepening

occurred due to the progression of the disease. The axial elevation map highlights the protrusion of corneal curvature.

This study uses axial maps divided into ten groups based on the Amsler–Krumeich standard classification scheme [38] that relies upon the anterior corneal features for the identification of keratoconus and its progression shown in Fig. 18.1 according to the degree of steepening and skewing of the curvature [39]. As per the standard classification, patterns are identified as (i) Round, (ii) Oval, (iii) Symmetric Bowtie (SB), (iv) Symmetric Bowtie with Skewed Radial Axes (SB/SRAX), (v) Asymmetric Bowtie with Superior Steepening (ASB/SS), (vi) Asymmetric Bowtie with Inferior Steepening (ASB/IS), (vii) Asymmetric Bowtie with Skewed Radial Axes (AB/SRAX), (viii) Superior Steepening (SS) (ix) Inferior Steepening (IS) and (x) Irregular for identifying the severity of the keratoconus. Out of these labels, 'IS' and 'AB/SRAX' show irregularities in corneal curvature, whereas 'SB/SRAX' and 'Oval' reveal symmetry in them. According to the classification scheme, various

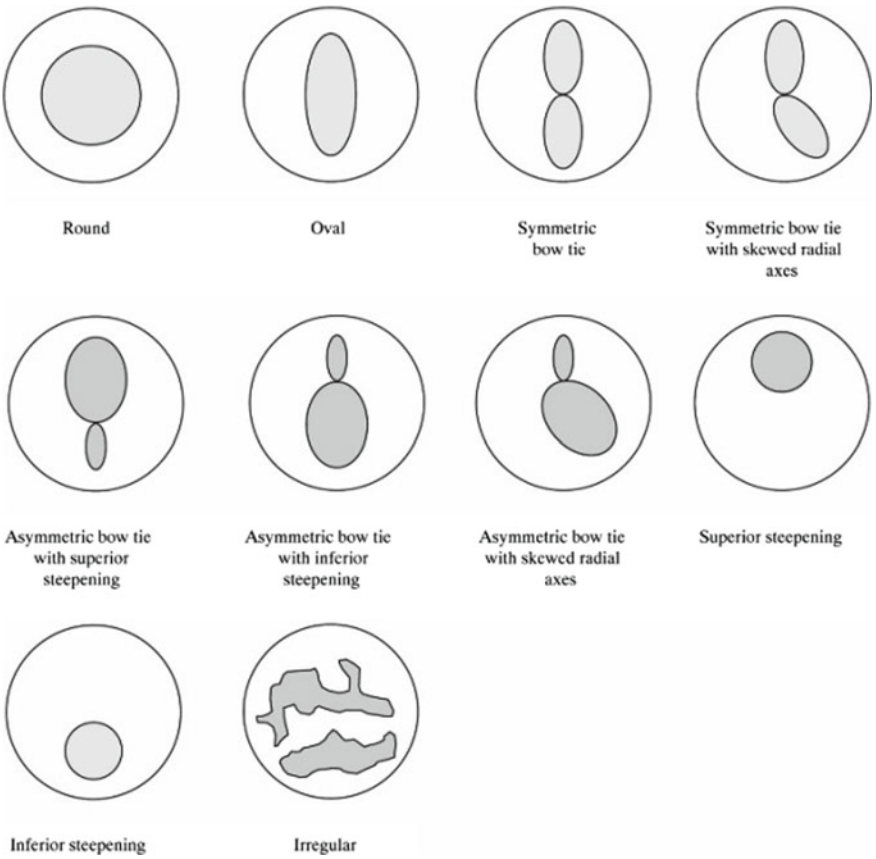

Fig. 18.1 Corneal topography pattern as per classification scheme [40]

patterns found due to the skewness occurred in corneal curvature were associated to the degree of progression of keratoconus [39]. Total 372 bilateral axial maps from 200 patients have been used as subject group, here in this study.

In our previous research, more than 800 maps of 534 × 534 × 3 pixels were processed with the methods of OpenCV to derive images with edges and area of steepening within edges from the elevation maps referred as 'images with edges and color mask'. There, we attained more than 98% of accuracy in detection of keratoconus from 'images with edges and color mask', variant of color topographical maps [41]. In continuation to our previous research, we selected 372 keratoconus images for all the ten classes in this study. This study excluded maps of forme fruste keratoconus. These selected maps were resized into 224 × 224 pixels in order to feed to our customized CNN model. Using transfer learning approach, the significant features were fed to the pretrained ImageNet models to form very deep layered learning architecture. Here, all 372 images were converted into grayscale eroded images with two objectives: (i) segregate the pattern from the images respect to the shape of the steepening and (ii) classify KCN images into ten varieties of shapes specified as per standard classification mentioned by Amsler–Krumeich by reducing the dimension of the derived images with images-and-mask [40].

The Computer Vision methods were used to achieve our first objective as follows. As a first step, the 'canny edge detection method' was customized to optimize the conversion of the color 'images with edges and mask' into grayscale eroded images. These RGB color images were converted into grayscale using OpenCV's color conversion method, followed by Gaussian method to eliminate the noise from the converted grayscale images. To determine any significant edge in an elevated area in an image, gradients were calculated using Sobel method of OpenCV. Further the double thresholding was applied to set the minimum and maximum threshold values. This was done to ultimately read the intensity of every pixel of the grayscale image to identify the most relevant pixel, for drawing an edge, pixel by pixel. Thus, initial requirement of deriving various shapes and patterns was successfully achieved by repeating the aforesaid steps on the data images which are shown in Fig. 18.2.

These derived shapes from the image were then used to determine the prevalence and type of the corneal distortion. For it, the grayscale images were required to be refined further, for determining the degree of the progression of keratoconus by classifying the shapes into ten labeled patterns as per Amsler–Krumeich standard classification scheme. These images were transformed into 64 × 64 to get convolved with Law's texture convolution method in order to reduce the dimension and refine the edges for clear identification of the shapes.

In this process, grayscale images were convolved with the five Law's texture energy kernels. These kernels are single dimensional, provide blurring of noise, smoothen the gray level texture, detect and contrast the edge and finally emphasize the ripples and spots at pixel level. Thus, the steepening patterns present in the maps were distinguished and were used further to check the bent of distortion in the curvature of the cornea. The grayscale eroded images can be further used for the classification of the patterns using the deep learning models.

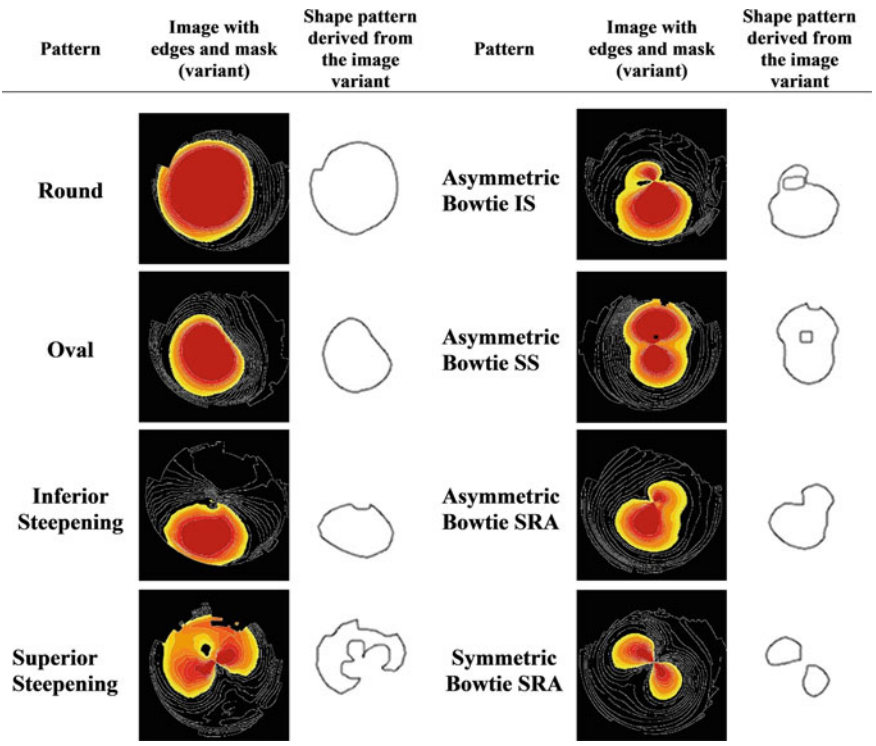

Fig. 18.2 Patterns from the variant of the keratoconus maps with edges and color mask

In order to attain the second objective of our study, the grayscale eroded images so obtained were used as an input. Also, here, we have used a wide range of conventional artificial neural network models, starting with ANN and also tried highly recommend deep neural network models which are ready-to-use and pretrained using millions of heterogeneous image datasets. Before feeding the image dataset to the various transfer learning models, highly imbalance maps in each of ten classes were further required to be augmented to balance the each class with sufficient data in it.

As shown in Fig. 18.3, new images were generated by augmenting with (i) rotation of 10 degree about height, (ii) width shift of 10% and (iii) horizontal and vertical flip. These steps yielded 3962 maps, amounting to approximately 350 images for each class. Here, the models used 3231 images for training and 359 as test data.

Figure 18.4 explains the workflow for the multiclass classification, wherein the preprocessed grayscale eroded images of corneal topographies with edges and mask were resized and used as an input for the ImageNet deep learning models. Various pretrained deep learning models were optimized using the transfer learning approach to classify the eroded maps into ten different groups. In this multiclass classification, the features were extracted from fully connected dense layer of models and then used them with logistic regression estimator as an input. These pretrained ImageNet

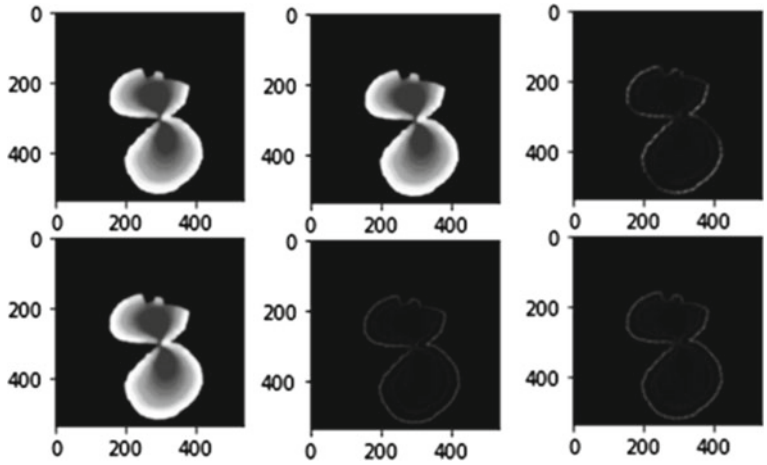

Fig. 18.3 Edges derived from eroded images using Law's texture method

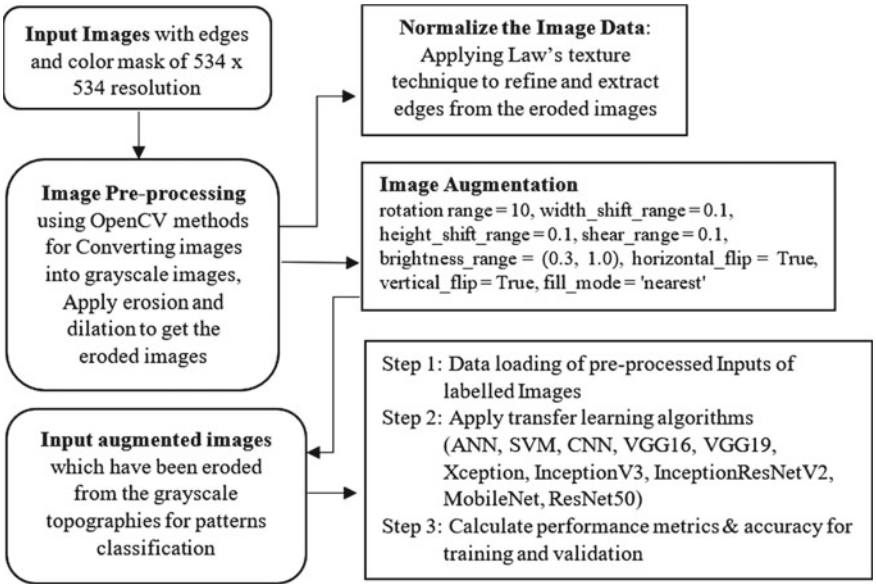

Fig. 18.4 Work flow of multiclass classification of topography patterns using images with edges and color mask

models are listed in Table 18.1 in Sect. 4, which were implemented using 'Keras module sets'.

Among the pretrained models used in this study, VGG16, VGG19, MobileNet and ResNet50 models use 224 × 224 for input images, whereas InceptionV3, Xception and InceptionResNetV2 demand 299 × 299 as input size. These architectures use

a large kernel size of 11 × 11 and 5 × 5, which are applied in the first couple of convolutional layers of the model, and the subsequent layers then use 3 × 3 sized kernel. Each of the selected pretrained deep convolutional neural network models used ImageNet weights with MaxPooling followed by single flatten layer and fully connected layer with two dense layers. 'ReLU' activation function was used by models to adjust the weights for assuring nonlinearity to convolutional layers. Also the default padding was used to fit the kernel over the images. A convolution layer followed MaxPooling layer to reduce the dimensionality of image and passing it to the next layer as an input. In order to implement transfer learning approach, sorted features from the first dense layer of fully connected were used to feed into logistic regression model to predict the probability ratio for each of the ten shapes. ANN model was designed with two dense layers of 256 and 128 neurons. After converting the output data into vector, it was fed to the fully connected layer which further used Softmax activation function to convert the output into probability indices. Batch normalization along with dropout method was applied in the subsequent layers after flattening to avoid overfitting.

Although the flattened layer could have measured the probability of significant features, yet we have applied the logistic regression upon the sliced fully connected layer to determine the various patterns to yield higher accuracy. We have selected VGG16, VGG19, InceptionResNetV2 and MobileNet networks, to achieve the aforesaid.

18.4 Discussion and Results

We had to erode the grayscale images so that it can be classified into various groups based upon corneal steepening patterns. Since ANN alone was not able to classify the preprocessed images into various classes and exhibited poor training and testing accuracy, we further trained our pretrained deep learning models by fitting the logistic regression estimator using the transfer learning approach to elevate the classification capabilities of each model. This would ultimately help us in determining the degree of progression of the keratoconus disease. VGG16 and VGG19 models used 4096 features. InceptionV3 and MobileNet models have used 1000 features. A total of 2048 features were used by ResNet50 model, while the InceptionResNetV2 used 1536 features only. Table 18.1 illustrates the comparative chart of the performance metrics. It was necessary for highlighting the quality of classification of patterns of corneal steepening, through transfer learning.

Among the pretrained models used here for classification, VGG16 and VGG19 gave 99.41% and 99.62% training accuracy, whereas the testing accuracy obtained by the same models was 76.04% and 77.43%, respectively. MobileNet and ResNet50 trained the model well with 91.95% and 92.23% accuracy and classified data with 75.48 and 76.60 test accuracy. The prediction by the Xception and InceptionV3 were 50.13% and 34.26%, respectively.

Table 18.1 Comparison of training accuracy and testing accuracy obtained by deep learning neural networks using transfer learning approach KCN grayscale topographic maps of KCN

Model type	Training accuracy	Testing accuracy	Precision	Recall	*F*1-score
ANN	20.73	12.26	–	–	–
VGG16	99.41	76.04	75.93	76.04	75.79
VGG19	99.62	77.43	77.59	77.43	77.38
Xception	63.75	50.13	51.02	50.13	50.03
InceptionV3	34.21	34.26	38.33	34.26	32.11
InceptionResNetV2	86.22	77.18	76.21	77.16	76.42
MobileNet	91.95	75.48	75.75	75.49	75.39
ResNet50	92.23	76.60	–	–	–

As it can be seen from the Table 18.1 that the performance of models—Xception and InceptionV3—was not up to the mark in spite of using the logistic regression for accuracy optimization; hence, the support vector machine was then applied with these two models to improve accuracy but resulted into 37.88% for Xception and 38.44% for InceptionV3 model, respectively, which were similar to the performance gained using logistic regression by these two models. InceptionResNetV2 exhibited 86.22% as training accuracy and 77.18% as testing accuracy which was closer to testing fit with better training to testing ratio. Out of many of applied transfer learning models, VGG16, VGG19, InceptionResNetV2 and MobileNet showed an assuring average of 76.24% *F*1-score. Thus, results with more than 75% accuracy in identifying the corneal steepening patterns are further illustrated in Table 18.1 herein.

18.5 Analysis of Results

Figure 18.5 gives the performance matrix attained by the various pretrained models used here, whereas Fig. 18.6 represents the comparison of the various training and testing accuracies gained by each of the deep convolutional models when applied upon keratoconus dataset.

Here, since the VGG16 and VGG19 were trained well, its training accuracy attained was 99.41% and 99.62%, respectively. However, VGG16's confusion matrix, in few cases, suggests that it misclassified the 'Asymmetric Bowtie - Inferior steepening' image with 'Asymmetric Bowtie – skewed radial axis' image. Similarly, VGG19, in few cases, mistook 'Asymmetric Bowtie – skewed radial axis' maps as 'Superior Steepening' image. In spite of such a great training accuracy, VGG16 and VGG19, testing accuracy came down to 76.04% and 77.43%, respectively.

The InceptionResiNetV2 led to well-balanced training and testing accuracy of 86.22% and 77.18%, respectively, when it comes to identification of corneal curvature. The MobileNet yielded 91.95% of training and 75.48% testing accuracy. The

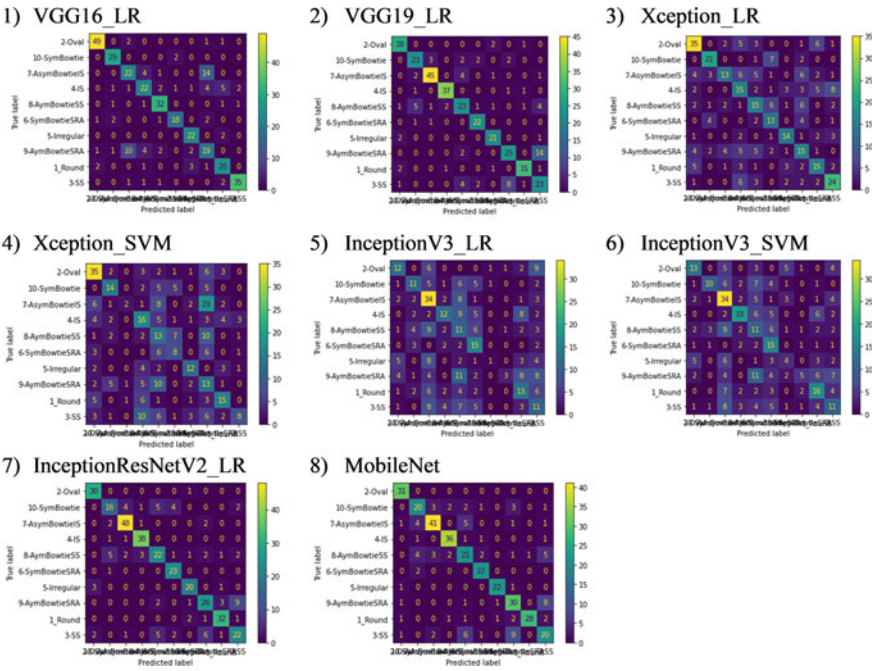

Fig. 18.5 Confusion matrix for each transfer learning model

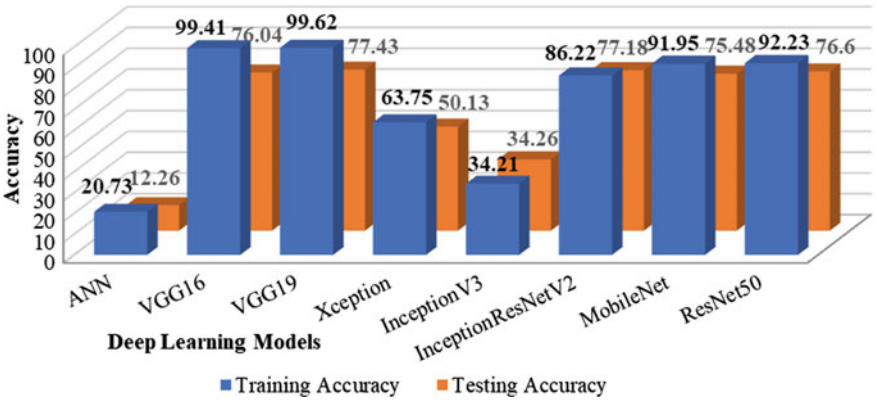

Fig. 18.6 Comparative analysis of the training and testing accuracies obtained by various deep learning models, when approached with the transfer learning

ResiNet50 obtained training and testing accuracy of 92.23% and 76.6%, respectively. It shall be noted from the Fig. 18.5 that even the very basic ANN, widely used Xception, which is extension of the Inception model and InceptionV3, these three

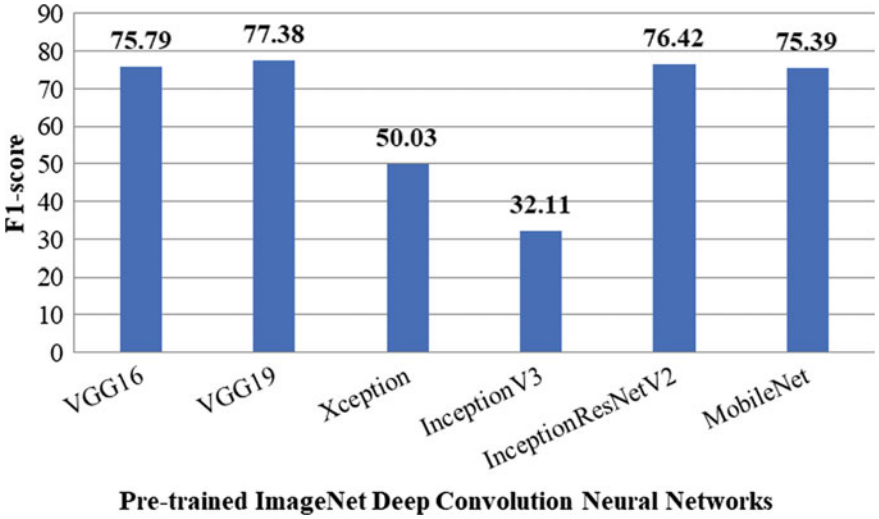

Fig. 18.7 *F*1-score of pretrained deep neural network model applied with eroded corneal maps

models out of many used here were highly unstable and their performance was below average.

The deep neural models used here were frequently misinterpreted the following two patterns, i.e., (i) manifestation due to occurrence of skewed steepening in the inferior side of cornea and (ii) 'Symmetric bowtie' shapes, that with the 'Round' and 'Oval' maps which often prevail in the advanced keratoconus.

Figure 18.7 shows the overall performances of all the deep neural models used herein, as per respective F1-scores as follows: the VGG19 had the highest of 77.38%, InceptionResNetV2 attained 76.42% and the VGG16's 75.79% and MobileNet's 75.39% were almost similar. However, the InceptionV3 and Xception were average in identifying the corneal steepening pattern accurately.

It can be seen in Fig. 18.8 that Xception and InceptionV3 have led to the highest misclassification followed by the VGG16. While VGG19 and MobileNet showed similar performances in classifying patterns, it was the InceptionResNetV2 that outperformed that too with minimal error rate.

Among all the pretrained models, with the eroded images of distorted corneal curvatures, the performance of InceptionResNetV2 was the best with minimum misinterpretation rate and was trained well with similar training and testing accuracy.

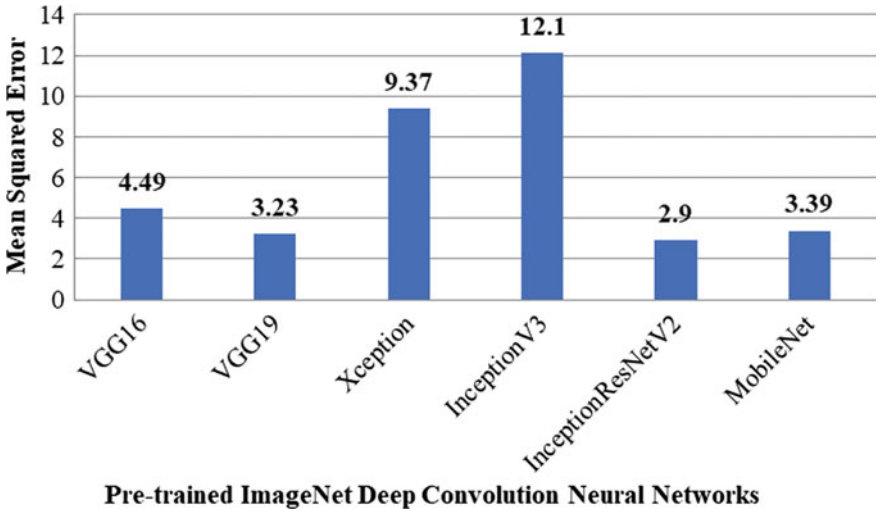

Fig. 18.8 MSE for pretrained deep neural network model applied with eroded corneal maps

18.6 Conclusion and Future Work

Out of our research, it can logically be concluded that the 'InceptionResNetV2, VGG19, MobileNet and VGG16 had best of accuracy, precision, Recall and F1-score', among all the pretrained models used herein with bilateral corneal axial maps for determining the keratoconus pattern. Hence any of the aforesaid, our researched, deep convolution neural networks can be used to identify the corneal steepening patterns to determine the keratoconus progression and its comparative treatments. However, the pattern classification was made using only anterior featured corneal maps. Even for refractive surgeries, our researched CNN, can be used along with the shapes classified using Law's texture. We hope our gathered knowledge of patterns and shapes of the distortion in corneal curvature will enable early detection of keratoconus, in times to come.

References

1. Romero-Jiménez, M., Santodomingo-Rubido, J., Wolffsohn, J.S.: Keratoconus: a review. Cont. Lens Anterior Eye **33**, 157–166 (2010)
2. Krachmer, J.H.: Keratoconus and related noninflammatory cornea1 thinning disorders. Surv. Ophthalmol. **30** (1984)
3. Piñero, D.P., Nieto, J.C., Lopez-Miguel, A.: Characterization of corneal structure in keratoconus. J. Cataract Refract. Surg. **38**, 2167–2183 (2012)
4. McComish, B.J., et al.: Association of genetic variation with keratoconus. JAMA Ophthalmol. **138**, 174 (2020)
5. Pedrotti, E., et al.: New treatments for keratoconus. Int. Ophthalmol. **40**, 1619–1623 (2020)

6. Dapena, I., Parker, J.S., Melles, G.R.J.: Potential benefits of modified corneal tissue grafts for keratoconus: Bowman layer 'inlay' and 'onlay' transplantation, and allogenic tissue ring segments. Curr. Opin. Ophthalmol. (Publish Ahead of Print) (2020)
7. Fariselli, C., Vega-Estrada, A., Arnalich-Montiel, F., Alio, J.L.: Artificial neural network to guide intracorneal ring segments implantation for keratoconus treatment. Eye Vis. **7**, 20 (2020)
8. Bejdic, N., Biscevic, A., Pjano, M., Ivezic, B.: Incidence of keratoconus in Refractive surgery population of Vojvodina—single center study. Mater. Sociomed. **32**, 46 (2020)
9. Salomão, M., et al.: Recent developments in keratoconus diagnosis. Expert Rev. Ophthalmol. **13**, 329–341 (2018)
10. Arbelaez, M.C., Versaci, F., Vestri, G., Barboni, P., Savini, G.: Use of a support vector machine for keratoconus and subclinical keratoconus detection by topographic and tomographic data. Ophthalmology **119**, 2231–2238 (2012)
11. Karabatsas, C.H., Cook, S.D., Sparrow, J.M.: Proposed classification for topographic patterns seen after penetrating keratoplasty. Br. J. Ophthalmol. **83**, 403–409 (1999)
12. Accardo, P.A., Pensiero, S.: Neural network-based system for early keratoconus detection from corneal topography. J. Biomed. Inform. **35**, 151–159 (2002)
13. Kreps, E. O., Claerhout, I. & Koppen, C. Diagnostic patterns in keratoconus. *Contact Lens and Anterior Eye* S136704842030103X (2020) doi:https://doi.org/10.1016/j.clae.2020.05.002.
14. Yu, Y., et al.: Deep transfer learning for modality classification of medical images. Information **8**, 91 (2017)
15. Shin, H.-C., et al.: deep convolutional neural networks for computer-aided detection: CNN architectures, dataset characteristics and transfer learning. IEEE Trans. Med. Imaging **35**, 1285–1298 (2016)
16. Kim, H.G., Choi, Y., Ro, Y.M.: Modality-bridge transfer learning for medical image classification. In: 2017 10th International Congress on Image and Signal Processing, BioMedical Engineering and Informatics (CISP-BMEI), pp. 1–5. IEEE (2017). https://doi.org/10.1109/CISP-BMEI.2017.8302286
17. Lu, W., et al.: Applications of artificial intelligence in ophthalmology: general overview. J. Ophthalmol. **2018**, 1–15 (2018)
18. Smolek, M.K.: Current keratoconus detection methods compared with a neural network approach. Invest. Ophthalmol. **38**, 10 (1997)
19. Kovács, I., et al.: Accuracy of machine learning classifiers using bilateral data from a Scheimpflug camera for identifying eyes with preclinical signs of keratoconus. J. Cataract Refract. Surg. **42**, 275–283 (2016)
20. Toutounchian, F., Shanbehzadeh, J., Khanlari, M.: Detection of keratoconus and suspect keratoconus by machine vision. Hong Kong **3** (2012)
21. Valdés-Mas, M.A., et al.: A new approach based on Machine Learning for predicting corneal curvature (K1) and astigmatism in patients with keratoconus after intracorneal ring implantation. Comput. Methods Programs Biomed. **116**, 39–47 (2014)
22. Smadja, D., et al.: Detection of subclinical keratoconus using an automated decision tree classification. Am. J. Ophthalmol. **156**, 237-246.e1 (2013)
23. Consejo, A., Melcer, T., Rozema, J.J.: Introduction to machine learning for ophthalmologists. Sem. Ophthalmol. **34**, 19–41 (2019)
24. Souza, M.B., Medeiros, F.W., Souza, D.B., Garcia, R., Alves, M.R.: Evaluation of machine learning classifiers in keratoconus detection from orbscan II examinations. Clinics **65**, 1223–1228 (2010)
25. Badillo, P.D., Zhivolupova, Y.A., Kudlakhmedov, S.Sh.: Convolutional neural networks for astigmatism detection. In: 2020 IEEE Conference of Russian Young Researchers in Electrical and Electronic Engineering (EIConRus), pp. 1360–1365. IEEE (2020). https://doi.org/10.1109/EIConRus49466.2020.9038998
26. Jmour, N., Zayen, S., Abdelkrim, A.: Convolutional neural networks for image classification. In: 2018 International Conference on Advanced Systems and Electric Technologies (IC_ASET), pp. 397–402. IEEE (2018). https://doi.org/10.1109/ASET.2018.8379889

27. Klyce, S.D.: The future of keratoconus screening with artificial intelligence. Ophthalmology **125**, 1872–1873 (2018)
28. Imran, A., et al.: Fundus image-based cataract classification using a hybrid convolutional and recurrent neural network. Vis. Comput. (2020). https://doi.org/10.1007/s00371-020-01994-3
29. Lavric, A., Valentin, P.: KeratoDetect: Keratoconus detection algorithm using convolutional neural networks. Comput. Intell. Neurosci. **2019**, 1–9 (2019)
30. Salih, N., Hussein, N.: Human Corneal state prediction from topographical maps using a deep neural network and a support vector machine. **8**
31. Kattire, S.S., Shah, A.V.: Boundary detection algorithm implementation for medical images. Int. J. Eng. Res. **3**, 3 (2014)
32. Litjens, G., et al.: A survey on deep learning in medical image analysis. Med. Image Anal. **42**, 60–88 (2017)
33. Kuo, B.-I., et al.: Keratoconus screening based on deep learning approach of corneal topography. Trans. Vis. Sci. Tech. **9**, 53 (2020)
34. Sonar, H., Kadam, A., Bhoir, P., Joshi, B.: Detection of keratoconus disease. ITM Web Conf. **32**, 03019 (2020)
35. Hesamian, M.H., Jia, W., He, X., Kennedy, P.: Deep learning techniques for medical image segmentation: achievements and challenges. J Digit Imaging **32**, 582–596 (2019)
36. Belin, M.W., Khachikian, S.S.: An introduction to understanding elevation-based topography: how elevation data are displayed—a review. Clin. Experiment. Ophthalmol. **37**, 14–29 (2009)
37. Martínez-Abad, A., Piñero, D.P.: New perspectives on the detection and progression of keratoconus. J. Cataract Refract. Surg. **43**, 1213–1227 (2017)
38. Giannaccare, G., et al.: Comparison of Amsler-Krumeich and Sandali classifications for staging eyes with keratoconus. Appl. Sci. **11**, 4007 (2021)
39. Li, X., Yang, H., Rabinowitz, Y.S.: Keratoconus: classification scheme based on videokeratography and clinical signs. J. Cataract Refract. Surg. **35**, 1597–1603 (2009)
40. Rasheed, K., Rabinowitz, Y.S., Remba, D., Remba, M.J.: Interobserver and intraobserver reliability of a classification scheme for corneal topographic patterns. Br. J. Ophthalmol. **82**, 1401–1406 (1998)
41. Gandhi, S.R., Satani, J., Bhuva, K., Patadiya, P.: Evaluation of deep learning networks for keratoconus detection using corneal topographic images. In: Singh, S.K., Roy, P., Raman, B., Nagabhushan, P. (eds.) Computer Vision and Image Processing, pp. 367–380. Springer, Singapore (2021)